

# Improvement of the microcapacitive humidity sensor by the package optimisation

Jihang Liu<sup>1,2</sup>, Lidong Du<sup>1</sup>, Ji Jin<sup>2</sup>, Zhen Fang<sup>1,2</sup>, Zhan Zhao<sup>1,2</sup> ✉

<sup>1</sup>State Key Laboratory of Transducer Technology, Aerospace Information Research Institute, Chinese Academy of Sciences, Beijing, People's Republic of China

<sup>2</sup>University of Chinese Academy of Sciences, Beijing, People's Republic of China

✉ E-mail: zhaozhan@mail.ie.ac.cn

Published in Micro & Nano Letters; Received on 30th June 2019; Revised on 18th November 2019; Accepted on 20th November 2019

To achieve good properties such as the hysteresis, repeatability, stability, linearity and response time in this work, the optimisation processes of the package are presented for a microcapacitive humidity sensor. On the basis of theoretical analysis, the optimisation will be conducted in two ways, including reducing the effect of parasitic capacitance in the microcapacitive humidity sensor measurement system and decreasing the adsorption of water molecules on the package surface. The reduction of the influence of parasitic capacitance was realised by reasonably designing the PCB and the isolation package. The decrease of water adsorption on the package surface was achieved by coating a layer of hydrophobic material. The experimental results proved that the package optimisation enables the humidity sensor with better performance; for instance the hysteresis error is more than six times lower, the repeatability error is more than ten times lower, and the temperature drift is about two times lower, and the linear fitting error is three times lower than the pre-optimised humidity sensor. Especially, the humidity response time in both adsorption and desorption is extremely improved.

**1. Introduction:** Due to the advantages of high sensitivity, high precision, and high stability, capacitive humidity sensors have been widely used in many fields: environmental humidity measurement, high altitude meteorological monitoring and the industry moisture-controlling [1–3]. Normally, in order to further improve the humidity response time and hysteresis characteristic, the capacitance is getting smaller and smaller nowadays [4–6]. The initial capacitance of the microcapacitive sensor is reduced down to 0–8 pF [7], which is the same order of magnitude as the parasitic capacitance, and sometimes even smaller. Hence, the parasitic capacitance can easily exert a severe influence on the humidity sensor's properties such as repeatability, linearity and hysteresis characteristics, etc. Therefore, it is of the most important to eliminate the effect of the parasitic capacitance for these microcapacitive sensors.

In the past two decades, a lot of research has been done to reduce the influence of parasitic capacitance. Some researchers explicitly analysed the role of porous silicon in the reduction of parasitic capacitance for humidity sensing [8]. Some other researchers focused on the high-sensitivity capacitive humidity sensor, in which the parasitic capacitances were decreased by special electrodes design and a SiO<sub>2</sub> layer introduction [9]. Furthermore, dielectric structure optimisation could also be used to reduce the parasitic capacitance for a CMOS-MEMS accelerometers chip, which resulted in the sensitivities being almost one order larger than the existing design [10]. In summary, all the above-mentioned methods were carried out from the point of the sensor structure.

In this Letter, we will improve the microcapacitive humidity sensor on two aspects: one is to reduce the effect of parasitic capacitance, and the other is to optimise its package. First of all, the microcapacitive humidity sensor was fabricated by the MEMS process, and the humidity sensor measurement system was developed. Then, we carried out the theoretical analysis on the package design of the printed circuit board (PCB) and the isolation shelter. Finally, a series of humidity response experiments were carried out. It was proved that with the package optimisation, we could obtain a high-precision, low-hysteresis, high-stability, and a fast-response sensor system. This also can provide a reference for the integrated design of a high precision microcapacitive humidity sensor.

## 2. Theory and experiment

**2.1. Design of the microcapacitance humidity sensor system:** The capacitive humidity sensor system was designed, as shown in Fig. 1. The structure of the sensor mainly contains three parts: a core capacitor, a heating resistor, and a temperature resistor. The capacitor consists of Pt bottom electrode (3), polyimide layer (4), and Pt top electrode (5). Heating resistor (6) and temperature resistor (7) are closely placed around the capacitor, which can be used to monitor and control the chip temperature accurately. When the Pt top electrode is designed with microholes, the water molecules would be easily adsorbed into the polyimide layer. Therefore, the capacitance shift, caused by the ambient humidity, could be measured by the detection circuit described below.

The schematic diagram of the interface detection circuit contains three functional modules: the humidity detecting module, the temperature detecting module, and the heating module. Among them, the capacitance detecting circuit based on the AD7745 chip was connected to the core capacitor for humidity measurement. The resistance detecting circuit based on the AD7793 chip was connected to the temperature resistor (180  $\Omega$ ) for temperature measurement. The heating resistor (60  $\Omega$ ) was connected directly to the MSP430 microcontroller chip for heating and moisture desorption. The sensor system is controlled by a computer.

**2.2. Analysing the effect of the parasitic capacitance in the sensor:** The principle of the capacitive humidity sensor is based on the Looyenga empirical formula. The dielectric constant  $\epsilon$  of the polymer film can be calculated as (1).  $\epsilon_f$  is the relative dielectric constant of polyimide, which is usually equal to 2.7 when the relative humidity is zero.  $\epsilon_w$  is the dielectric constant of water vapour, which can be described as follows:

$$\epsilon = [\gamma(\epsilon_w^{1/3} - \epsilon_f^{1/3}) + \epsilon_f^{1/3}]^3 \quad (1)$$

$$\epsilon_w = 78.54[1 - 4.6 \times 10^{-4}(T - 298) + 8.8 \times 10^{-6}(T - 298)^2] \quad (2)$$

where  $T$  is the absolute temperature of the environment,  $\gamma$  is the diffusion volume ratio of water molecules in the polymer film, which is determined by Fick's diffusion law [11]. Hence, the ideal

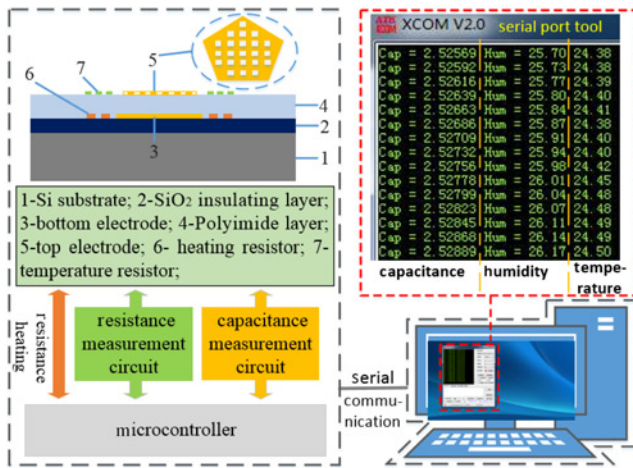


**Fig. 1** Schematic diagram of the MEMS capacitive humidity sensor measurement system

capacitance value can be calculated by (3),  $\epsilon_0$  is the permittivity of vacuum,  $A$  and  $d$  are the electrode area and distance, respectively.

$$C_s = \frac{\epsilon_0 A}{d} \times \epsilon \quad (3)$$

Theoretically, the capacitance detection circuit is designed for obtaining the variation of capacitance  $C_s$  with humidity change. However, there always are a lot of parasitic capacitors that are introduced in the detection loop inevitably. In practice, the equivalent circuit of the capacitance detection loop was separated from the system and then established, as shown in Fig. 2. All parasitic factors affecting the output of the core capacitor were considered, including the edge parasitic capacitance, pad parasitic capacitance, bonding wire capacitance, pin parasitic capacitance, and the detection circuit capacitance.

In Fig. 2,  $R_p$  is a parallel loss resistor, which represents the leakage resistance and the dielectric loss between the top and bottom electrodes. The effect of this part is usually larger at low frequencies,  $R_s$  is the series resistance, which represents the resistance of the wire, the resistance of the capacitor electrodes and the support layer. It is usually negligible when operating at low frequencies. The inductance  $L$  is composed of the inductance of the capacitor itself and the inductance of the external lead. The former is related to the capacitor structure, and the latter depends on the length of the wire.  $C_p$  is the summary of all the parallel parasitic

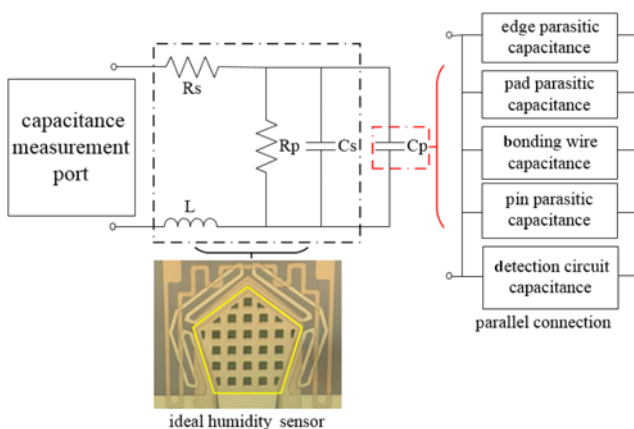


**Fig. 2** Analysis of all factors affecting the output of the capacitive humidity sensor

factors whose first two items could be considered in humidity sensor design. Among all of the parasitic capacitance, the former two items are related to the capacitor structure, which is minor influenced by the ambient humidity. The latter two items are related to the circuit and the isolation package. They would be seriously affected by the ambient humidity. For instance, the capacitance among pins and the detection circuit can be equivalent to an extra unstable humidity sensor due to the coverage of another polymer material. The worst of it is that this unstable part has no short-term repeatability. Hence, we should avoid using the connecting pins and shorten the detection circuit. To reduce the influence of the last three items, we would optimise the design of the PCB capacitance measurement circuit and the isolation protection of the package.

**2.3. Experiment design:** First, the microcapacitive humidity sensor chip was bonded on the PCB. The system was prepared according to the schematic diagram above. An optimised sample was designed by removing the pins and shorting the wire distance through vias. For comparison, we also developed an original sample in which pins were adopted to connect the separated humidity sensor. Then, the isolation package was also implemented for the optimised sample, as shown in Fig. 3, and it was fabricated by 3D printing technology. Moreover, in order to improve the response time of this system, we further treated the isolation package by the hydrophobic solution (GF-2200) (Dongguan Guangfu Chemical Co., Ltd) for 24 h at 25°C. The effect was characterised by a contact angle test and the results were discussed in the next section.

Finally, the humidity generator (Model 2000, USA) was used for the humidity response test. And the high-low temperature alternating test chamber (GTHJ-C415010, CHN) was adopted for calibration. To analyse the effect of humidity, specially, we set the temperature to 25°C, and adjusted the relative humidity range between 15 and 85% RH.

**3. Result and discussion:** The humidity response curves are shown in Fig. 4a. It is illustrated that the capacitance of the optimised sample is 2.40828 pF, about half of the original sample 5.6524 pF. We can know that the parasitic capacitance introduced by the pins and wire in the detection circuit is almost 3.2 pF, even larger than the capacitance of the humidity sensitive part.

The hysteresis error, which is an essential factor for the humidity sensor, can seriously influence the accuracy. It can be calculated by (4) that the maximum humidity hysteresis error of the original sample is 2.02% RH, whereas, for the optimised sample, the maximum hysteresis error is reduced to 0.3% RH, which is

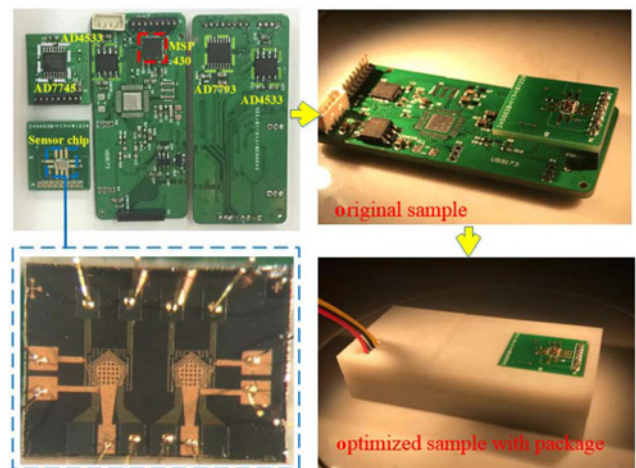


**Fig. 3** Micro-capacitive humidity sensor chip and the original sample and the packaged sample

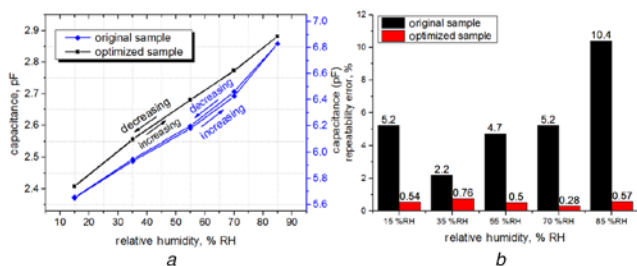


**Fig. 4** The optimization of hysteresis and repeatability  
*a* Hysteresis error comparing between the original sample and the optimised sample  
*b* Repeatability error of both the original sample and the packaged sample

improved more than six times

$$\xi_H = (RH_H - RH_L) \frac{|\bar{y}_{ad} - \bar{y}_{di}|_{\max}}{y_{FS}} \times 100\% \quad (4)$$

where  $\xi_H$  is the hysteresis error,  $RH_H$  and  $RH_L$  are the upper and lower relative humidity limits,  $\bar{y}_{ad}$  and  $\bar{y}_{di}$  are the average response capacitances of the adsorption and desorption, respectively.  $y_{FS}$  represents the whole offset of the humidity capacitance.

To achieve the repeatability error, we tested each sample for ten times. The results have been calculated by the ratio of the capacitance shift error to its full scale, as shown in Fig. 4b. Obviously, the optimisation is significant. The repeatability error of the optimised sample (<0.8%) is far less than that of the original sample (>10%), and it is improved by more than ten times.

It is widely acknowledged that the temperature can severely influence the measurement of humidity sensors. The original sample and the optimised sample were tested under 20, 25, 30, and 35°C, respectively, as shown in Fig. 5. The max capacitance shift of the original sample caused by temperature is 5.6% between 20 and 35°C, whereas, for the optimised sample, the max capacitance shift is decreased to 2.9%, which is improved about two times.

The linearity was also compared for these samples, as shown in Figs. 6a and b. Obviously, the linearity of the sensor is improved after the optimisation, and the fitting error is decreased from 4.5 to 1.4% RH, which is improved three times.

In addition, the response time is one of the most important factors for humidity sensors, which would be affected mainly by the characteristics of the package surface. So, for further improving its response time, the package surface should be changed from hydrophilic to hydrophobic. The effect was characterised by the liquid contact angle before and after the hydrophobic solvent treatment. 5  $\mu$ l deionised water was dropped on the package surface and observed through a high power stereo-microscope. It can be seen in Fig. 7 that the contact angle for the package surface is changed from 67° to 102° after being processed by the hydrophobic solvent. As

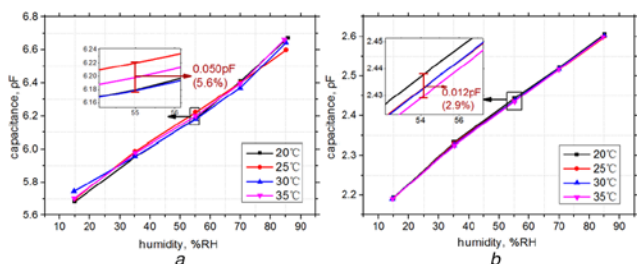


**Fig. 5** The humidity response at different temperature  
*a* Humidity response curves of the original sample  
*b* Humidity response curves of the optimised sample

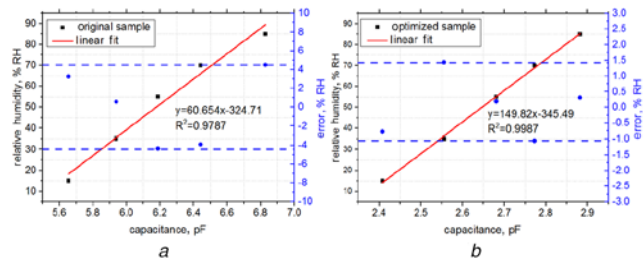


**Fig. 6** The linear fit of sensors  
*a* Linear fit of the original sample and its fitting error  
*b* Linear fit of the optimised sample and its fitting error

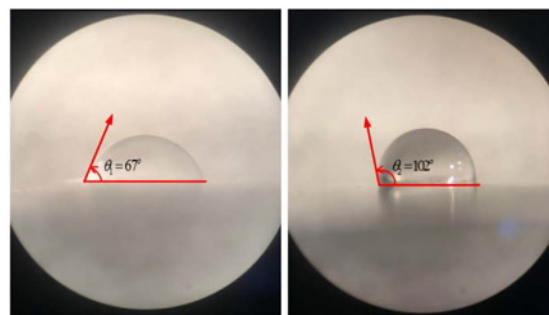


**Fig. 7** Liquid contact angle for the package surface before and after treatment on the left and on the right, respectively

expected, the hydrophilic surface of the package transformed into the hydrophobic one.

For obtaining the response time of the hydrophilic package sample and the hydrophobic package sample, we tested the optimised sample with or without treatment by the hydrophobic solvent in adsorption and desorption processes, respectively. In which, the ambient humidity range was set from 15 to 85% RH at 25°C, as shown in Fig. 8.

As expected, the response times corresponding to 63 and 90% water adsorption, respectively, are 14 and 37.5 s for the hydrophilic package sample, whereas it is just 10.5 and 28 s for the hydrophobic package sample. Similarly, the response times corresponding to 63 and 90% water desorption is 26 and 130 s for the hydrophilic package sample, whereas it is shortened to 19 and 58 s for the hydrophobic package sample. Obviously, both the adsorption and desorption response time are extremely improved due to the hydrophobic package surface.

For the solid surface, the distribution of water molecules depended on the characteristics of the surface and the ambient water molecule concentration. If the adsorption rate was higher than the desorption rate, the overall performance would show the net adsorption; conversely, it would be defined as the net

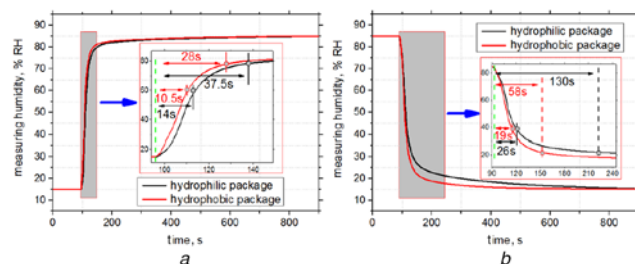


**Fig. 8** The response time comparing  
*a* Adsorption response comparing  
*b* Desorption response comparing



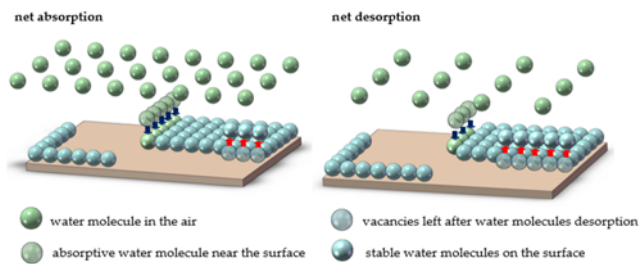


**Fig. 9** Dynamics of water molecules on the solid surface

**Table 1** Characteristics summarised for the original sample and optimised sample

Characteristics of the samples	Original sample	Optimised sample
hysteresis error	2.02% RH	0.3% RH
repeatability error	10.4% RH	0.76% RH
temperature error (20–35°C)	5.6%	2.9%
linear fitting error	4.5% RH	1.4% RH

**Table 2** Characteristics summarised for the hydrophilic package sample and the hydrophobic package sample

Response time of samples	Hydrophilic package	Hydrophobic package
63% complete adsorption	14 s	10.5 s
90% complete adsorption	37.5 s	28 s
63% complete desorption	26 s	19 s
90% complete desorption	130 s	58 s

desorption, as shown in Fig. 9. When the humidity sensor was packaged, the sensor and the package surface were set in the same experimental atmosphere. If the ambient humidity changed, the water molecules on each of them would dynamically and simultaneously change. So, there is a lot of competition between the humidity sensor and the package surface in this short term, which may seriously influence the response time of the sensor. According to the comparison of the response time between the hydrophilic package sample and the hydrophobic package sample, the hydrophobic surface would reduce the competition between the humidity sensor and the package efficiently.

In summary, most of the significant characteristics of the micro-capacitive humidity sensor can be improved by avoiding the influence of the parasitic capacitance. For comparison, we summarised the characteristics of the original sample and the optimised sample in Table 1.

Moreover, the response time of the sensor system can be improved by the hydrophobic package. For comparison, we summarised the characteristics of the hydrophilic package sample and the hydrophobic package sample in Table 2. It can be seen that a humidity sensor with the hydrophobic package could gain a shorter response time for either adsorption and desorption, this design may be promising for the fast-response humidity sensor in the special situation such as the meteorological observations in the atmospheric boundary layer [12] and respiration monitoring for human health [13], etc.

**4. Conclusion:** In this Letter, the optimisation processes of the package are presented for a microcapacitive humidity sensor. The reduction of the influence of parasitic capacitance was realised by reasonably designing the PCB and the isolation package, resulting in a lot of improvements for the sensor system: the hysteresis error is more than six times lower, the repeatability error is more than ten times lower, the temperature drift is about two times lower and the linear fitting error is three times lower than the pre-optimised humidity sensor. The decrease of water adsorption on the isolation package surface was achieved by coating the layer of a hydrophobic material with which improvement of the humidity response time was reached in both adsorption and desorption for the sensor system. It is proved by the experimental results that the package optimisation enables the humidity sensor with better performance and a good reference for designing and fabricating the high-precision, high-stability, and fast-response microcapacitive humidity sensor.

**5. Acknowledgments:** This work was supported by the National Natural Science Foundation of China (grant no. 61871363).

## 6 References

- [1] Mason A., Yazdi N., Najafi K., *ET AL.*: 'A low-power wireless micro-instrumentation system for environmental monitoring', Stockholm, Sweden, 1995, pp. 107–110
- [2] Luo Y., Kun Y., Shi Y., *ET AL.*: 'Research of radiosonde humidity sensor with temperature compensation function and experimental verification', *Sens. Actuators A*, 2014, **218**, (January), pp. 49–59
- [3] Wernecke R., Wernecke J.: 'Industrial moisture and humidity measurement: a practical guide' (Wiley, New Jersey, USA, 2014)
- [4] Zargar Z.H., Islam T.: 'A thin film porous alumina based cross-capacitive humidity sensor', *IEEE Trans. Instrum. Meas.*, 2019, PP, (c), pp. 1–1
- [5] Starke E., Turke A., Krause M., *ET AL.*: 'Flexible polymer humidity sensor fabricated by inkjet printing Technische Universität Dresden'. 2011 16th Int. Institute of Semiconductors and Microsystems, 01062 Dresden, Germany/Solid-State Sensors, Actuators Microsystems Conf. (TRANSDUCERS), Beijing, People's Republic of China, 2011, pp. 1152–1155
- [6] Guo R., Tang W., Shen C., *ET AL.*: 'High sensitivity and fast response graphene oxide capacitive humidity sensor with computer-aided design', *Comput. Mater. Sci.*, 2016, **111**, pp. 289–293
- [7] Lazarus N., Bedair S.S., Lo C.C., *ET AL.*: 'CMOS-MEMS capacitive humidity sensor', *J. Microelectromech. Syst.*, 2010, **19**, (1), pp. 183–191
- [8] Das J., Hossain S.M., Chakraborty S., *ET AL.*: 'Role of parasitics in humidity sensing by porous silicon', *Sens. Actuators A*, 2001, **94**, (1–2), pp. 44–52
- [9] Tsai M.H., Sun C.M., Liu Y.C., *ET AL.*: 'Design and application of a metal wet-etching post-process for the improvement of CMOS-MEMS capacitive sensors', *J. Micromech. Microeng.*, 2009, **19**, (10), pp. 1–7
- [10] Liu J., Du L., Pan Y., *ET AL.*: 'Reducing the effect of parasitic capacitance on the micro-capacitive humidity sensor'. Proc. of the 14th Annual IEEE Int. Conf. on Nano/Micro Engineered and Molecular Systems, Bangkok, Thailand, 11–14 April 2019, pp. 494–497
- [11] Laconte J., Wilmart V., Flandre D., *ET AL.*: 'High-sensitivity capacitive humidity sensor using 3-layer patterned polyimide sensing film'. SENSORS, 2003 IEEE, Toronto, Ont., 2003, pp. 372–377
- [12] Varentsov M.I., Artamonov A., Pashkin A.D., *ET AL.*: 'Experience in the quadcopter-based meteorological observations in the atmospheric boundary layer', *IOP Conf. Ser. Earth Environ. Sci.*, 2019, **231**, (1), p. 012053
- [13] Jiang B., Bi Z., Hao Z., *ET AL.*: 'Graphene oxide-deposited tilted fiber grating for ultrafast humidity sensing and human breath monitoring', *Sens. Actuators B Chem.*, 2019, **293**, (February), pp. 336–341